RESEARCH REPORT

VTT-R-08100-09

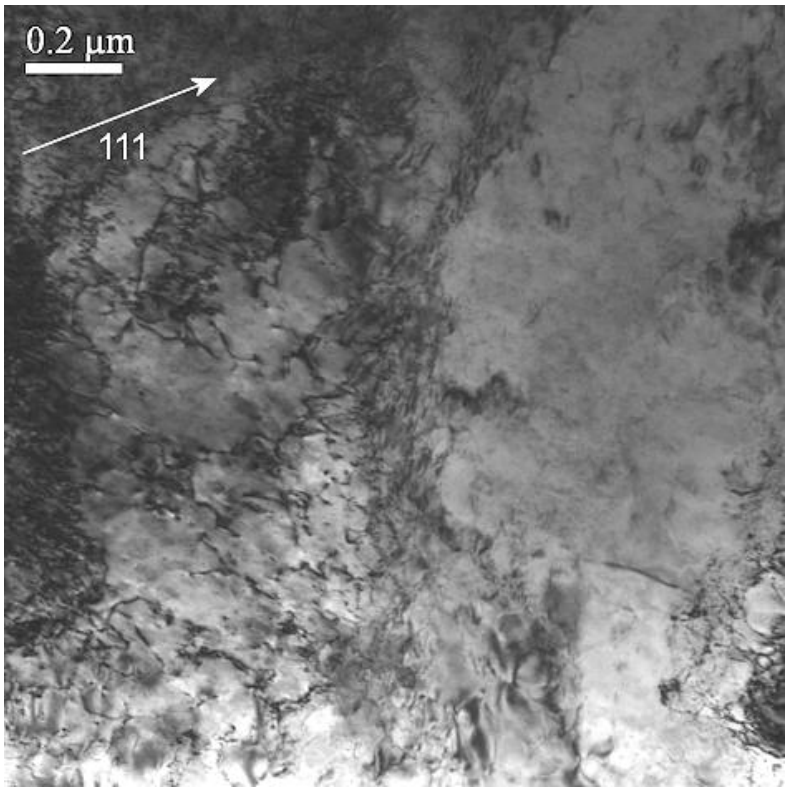

TEM microstructures of copper following three different EAC tests

Authors: Wade Karlsen, Janne Pakarinen

Confidentiality: Public

Report's title	
TEM microstructures of copper following three different EAC tests	
Customer, contact person, address Pertti Aaltonen, Kim Wallin	Order reference
Project name Kim Wallin Academy of Finland	Project number/Short name 36468/SA KWAK
Author(s) Wade Karlsen, Janne Pakarinen	Pages 22/
Keywords TEM, EAC, copper	Report identification code VTT-R-08100-09

Summary

In the selective dissolution, vacancy creep model it is postulated that corrosion processes at a material surface can, in some conditions, result in an overall net increase in vacancy flux from the oxide into the bulk metal. Vacancy injection is expected to promote dislocation activity, and subsequent dynamic recovery would be expected to soften the material locally. This could be viewed as a key precursor process for stress corrosion crack initiation. The goal of the current study was to utilize transmission electron microscopy (TEM) to examine the dislocation microstructure of tested materials following different test outcomes, in order to determine whether or not dislocation activity was significantly different following different test sequences.

Three different test bars were subjected to different combinations of strain and electrochemical polarization in EAC tests. TEM examinations conducted from different regions of the three test bars, each corresponding to a different combination of stress and environment, found only some differences between them. In all cases the majority of the microstructure in each specimen was comprised of a heavily distorted lattice bearing a high density of dislocations organized as dense mats of closely spaced, parallel dislocations. However, some localized regions appeared to exhibit a marked absence of dislocations, generally bounded by distinct boundaries, but still showing 100% copper in analyses. In a qualitative sense it seemed that the specimens from test bar loaded to 320 MPa (exceeding the nominal yield strength of the material) exhibited the most incidences of such dislocation-free grains, being found in all three deformed regions examined. On the other hand, while one specimen from the deformed material of the bar loaded at 250 MPa clearly showed the most dramatic, widespread incidence of such dislocation-free regions, similar regions were difficult or impossible to find in other specimens from deformed material in the same test bar. Meanwhile, at least one such region was also found in the gauge region of the test bar that was loaded at only 50 MPa, and therefore not expected to exhibit much deformation.

Calculations show that is possible that the predicted vacancy injection and subsequent vacancy/dislocation interactions may have occurred only at the immediate surface of the specimen though, so preparation of additional specimens focused only on the immediate subsurface region could enable observations that would more closely match what was expected.

Confidentiality	Public

Espoo, 27.11.2009

Written by	Reviewed by	Accepted by
Wade Karlsen Senior Research Scientist	Pertti Aaltonen Senior Research Scientist	Stefan Holmström Deputy Technology Manager

VTT's contact address
Kemistintie 3, Espoo; P.O. Box 1000, FI-02044 VTT, Finland

Distribution (customer and VTT)
Academy of Finland, VTT

Contents

1 Introduction

In the selective dissolution, vacancy creep model it is postulated that corrosion processes at a material surface can in some conditions result in an overall net increase in vacancy flux from the oxide into the bulk metal. When the bulk metal is under stress, vacancies injected in this manner are then expected to preferentially migrate to dislocations, where they are annihilated. The annihilation of vacancies at dislocations can promote creep processes in loaded material by enabling dislocation climb, manifested as material softening. At the same time, annihilation of vacancies maintains the vacancy concentration gradient, thereby maintaining the corrosion processes that would otherwise stop when a new vacancy equilibrium were reached.

There are many different mechanistic approaches or models to describe environmental-assisted cracking (EAC). In order to test the selective dissolution, vacancy creep model, specific tests have been developed using highly cold-worked, commercially pure copper, whereby a test bar submerged in appropriate solution is simultaneously subjected to a very slow but dynamic rising displacement and an increasing electrochemical polarity. Whereas during a particular test the load increase is nil, the overall load on the order of 320 MPa corresponds to the flow stress for the material, meaning that some sources would be expected to generate new dislocations, and thereby transmit a strain response in the material.

For the series of this study the electrochemical treatment was the same for all samples. The electrochemical sequence tends to create conditions where the sample surface is covered with Cu_2O type oxide, and later, at slightly higher potential, some CuO starts to precipitate on it. In this situation the anodic current passing through the oxide should provide vacancies to the bulk metal beneath the oxide, because the anodic electric current is due to Cu^+ ions and electron holes (mixed conductivity). It is expected that this can happen only at the potential range where Cu^{++} can exist before CuO precipitation starts. Due to vacancy generation and dislocation activity, deformation is expected to localize and the processes to start to sustain each other, which would be manifested in the load curve as material softening. This can be viewed as a key precursor process for stress corrosion crack initiation.

The goal of the current study was to utilize transmission electron microscopy (TEM) to examine the dislocation microstructure of tested materials following different test outcomes, in order to determine whether or not dislocation activity was significantly different following different test sequences.

2 Experimental Materials and Methods

<u>Cu reference sample</u>
The material is commercially pure copper. The material composition report is shown in Figure 1. It has been heavily cold worked and the dislocation density would be expected to be very high. The yield strength is about 250 MPa, and therefore the corresponding ideal cell size could be about 200 nm.

	Hapeton kupari OFE	Happikupari ETP
O	1,2	75
Ag	11	11
Al	0,34	0,6
As	0,43	1,4
Bi	0,09	0,64
Cd	<0,01	<0,01
Co	<0,03	<0,03
Fe	0,4	0,2
Mn	<0,1	<0,2
Ni	<0,4	1,5
P	<0,4	<0,4
Pb	1	0,79
S	3,8	4,6
Sb	0,06	0,27
Se	0,1	0,8
Si	0,3	1,2
Sn	0,05	0,34
Te	0,07	0,65
Zn	<0,2	<0,2
Zr	0,2	<0,1

Molemmat ovat siis varsin puhdasta materiaalia, kuparipitoisuus on 99.998 %. Ainut merkittävä ero on happipitoisuudessa.

Figure 1: Analysis results for the material

There were three different test bars chosen for TEM examination, each having been subjected to a slightly different combination of strain and electrochemical polarization in the corrosive solution. The polarization plots for each test are shown in Figure 2.

Cu8 sample (red curve):
The stress level in this sample (320 MPa) was high enough to support dislocation mobility. As shown in Figure 3, the polarization curve indicated a transition between Cu_2O and CuO, occurring simultaneous with a detectable, abrupt load drop, suggesting a sudden, rapid strain response in the material in that regime.

Cu6 sample (green curve):
Pits were visible after testing, which can be formed at higher potentials and therefore may not be relevant. However, the electrochemical current displayed fluctuations during the test, and perhaps the lower stress level and the limited mobility of dislocations in comparison to Cu8 sample could not support deformation localization. Instead, pitting may have occurred, which is usually considered to be solely an electrochemical phenomenon.

Cu5 sample (blue curve):
This sample behaved like any other non-strained bulk specimen. It passivated at a potential where CuO is expected to precipitate on the sample surface. The dislocation structure, even adjacent to the oxide film, would be expected to correspond to that of the reference sample.

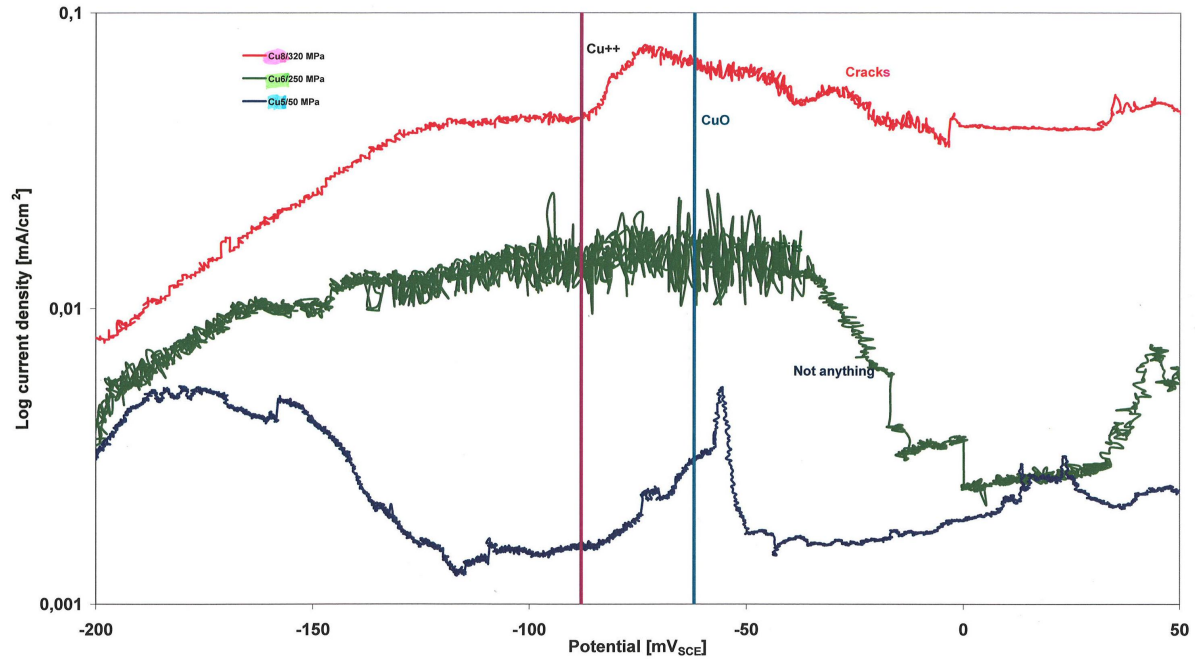

Figure 2: Current densities at different stress levels.

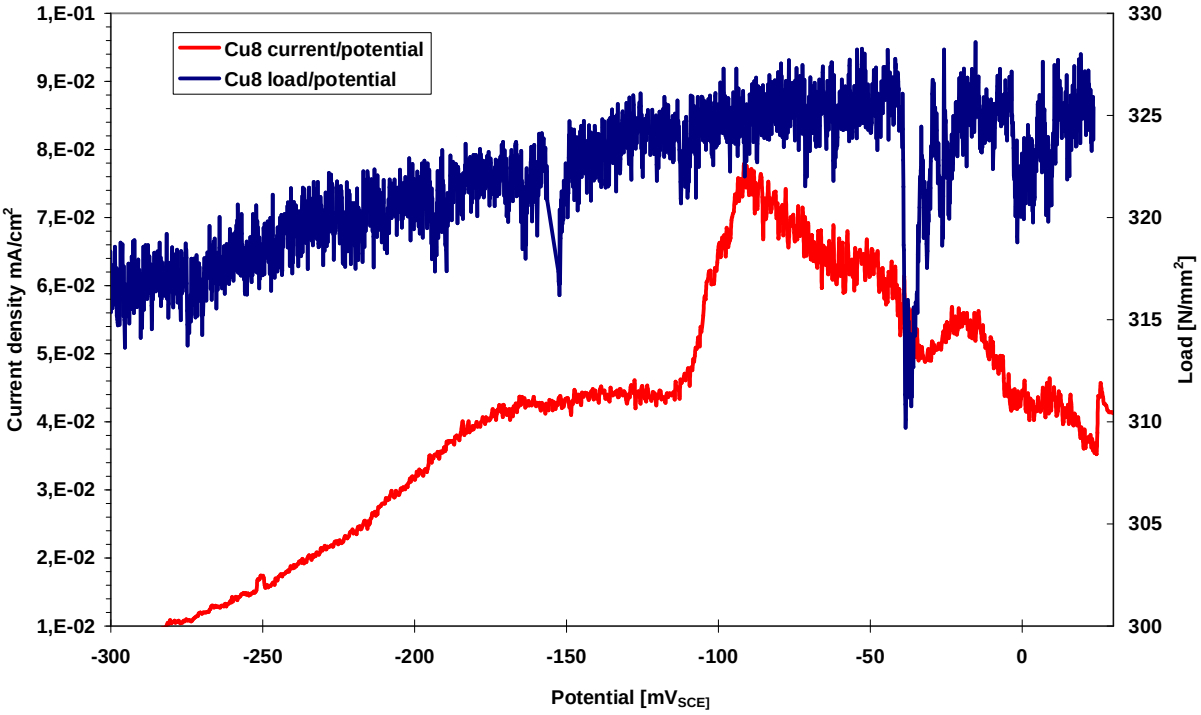

Figure 3: Load and current density at different potentials in specimen Cu8.

The test bars were designed with an hourglass shape in order to promote strain localization at the narrowest region of the specimen. However, in very slow EAC tests, crack-like features sometimes also appeared in the wider portion of the bar outside of the gauge region but still exposed to the environment. Therefore, blank disks for TEM specimen productions were extracted from different regions of the test bars, to assure sampling of microstructures within the different scenarios. The particular locations are shown as dotted-line circles in Figure 4. Each location was numbered, so a particular specimen was identified with the bar number followed by disk number, as Cu5_6, Cu6_1, etc.

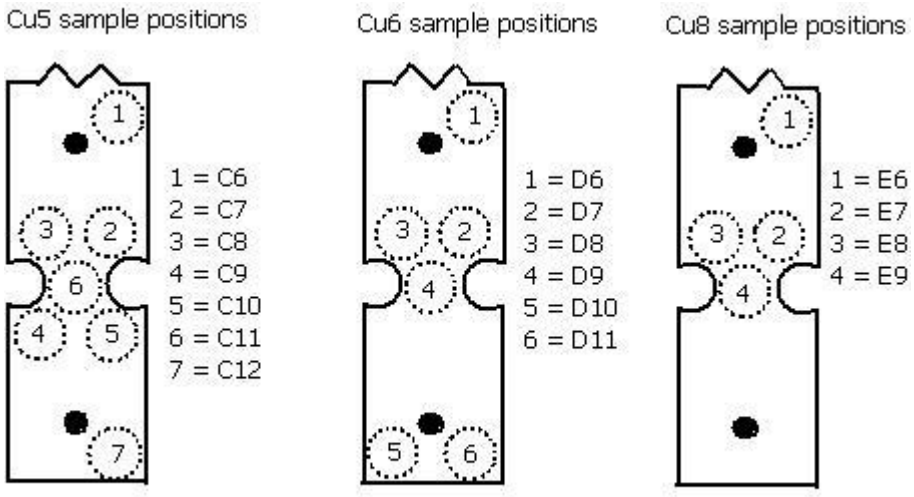

Figure 4: TEM specimen extraction locations from the three test bars.

Because any interaction between the corrosion-induced vacancies and dislocations would be expected to be most significant close to the test-bar surface, specimens were mechanically thinned only from one side. Thus, the original 1 mm-thick test bar was first ground to under 0.5 mm thick, the blanks were punched from it, then each blank was further precision-ground from that same side to the final blank thickness of <0.1 mm thick. This blank was subsequently electropolished to electron transparency from *both* sides in a solution of 20% nitric acid-methanol solution, at about -40°C and with a voltage of +9V. Assuming uniform material removal from each side, the examined material would correspond to a depth of about 50 microns from the original test bar surface that had been exposed to the environment during the test.

3 Results

A few stereomicroscope images were available of the test bars before TEM specimen extraction commenced. As shown in Figure 5, when loaded by only 50 MPa, the surface of the specimen had turned black. As shown in Figure 6, when loaded to 250 MPa some corrosion product and pitting were visible on the surface, though the test bar was still mostly copper coloured. Finally, as shown in Figure 7, at 320 MPa some features appeared on the specimen which could be interpreted to be cracks, despite occurring outside of the gauge region. A higher magnification image of those features is shown in Figure 8.

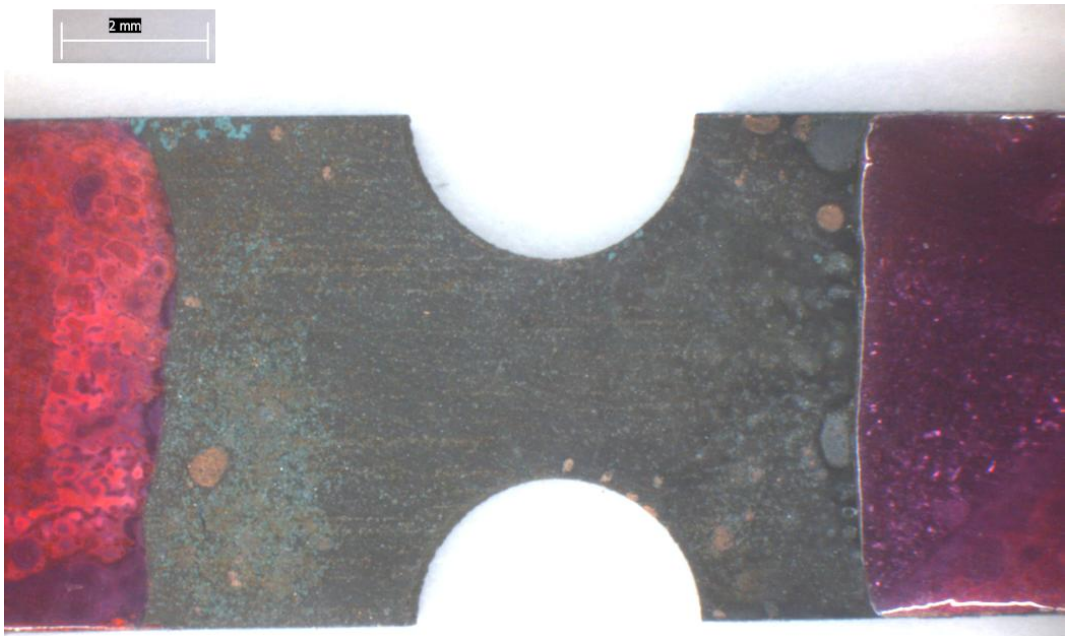

Figure 5: Stereomicroscope image of bar Cu5, which had been tested at a constant load of 50 MPa.

Figure 6: Stereomicroscopy image of bar Cu6, which had been tested at a constant load of 250 MPa.

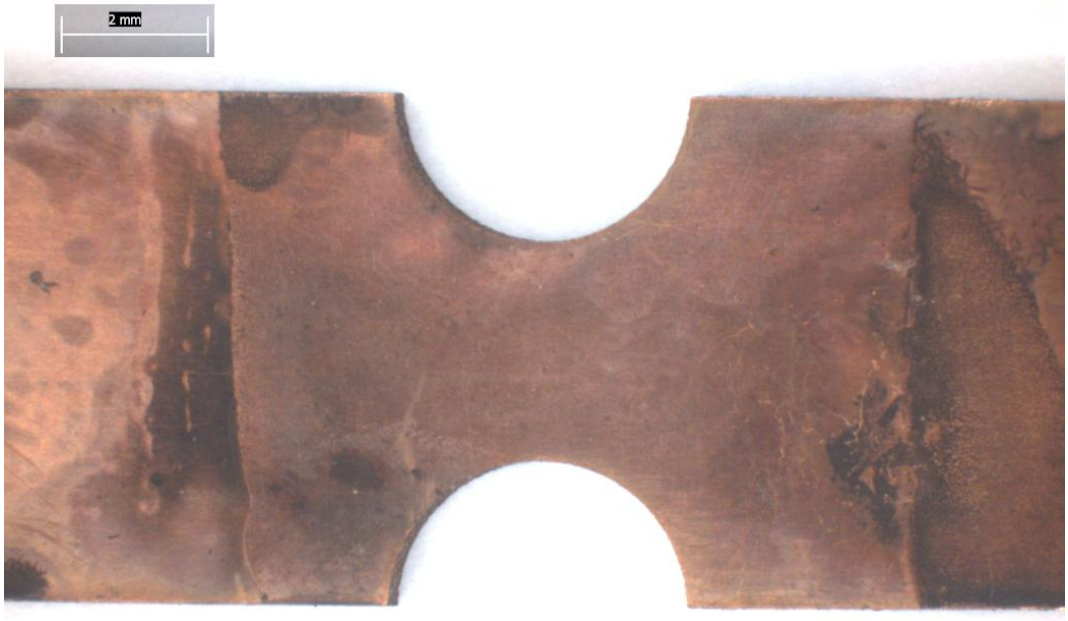

Figure 7: Stereomicroscope image of bar Cu8, tested at a constant load of 320 MPa. On the right-hand side of the bar are some features said to be cracks initiated during the test.

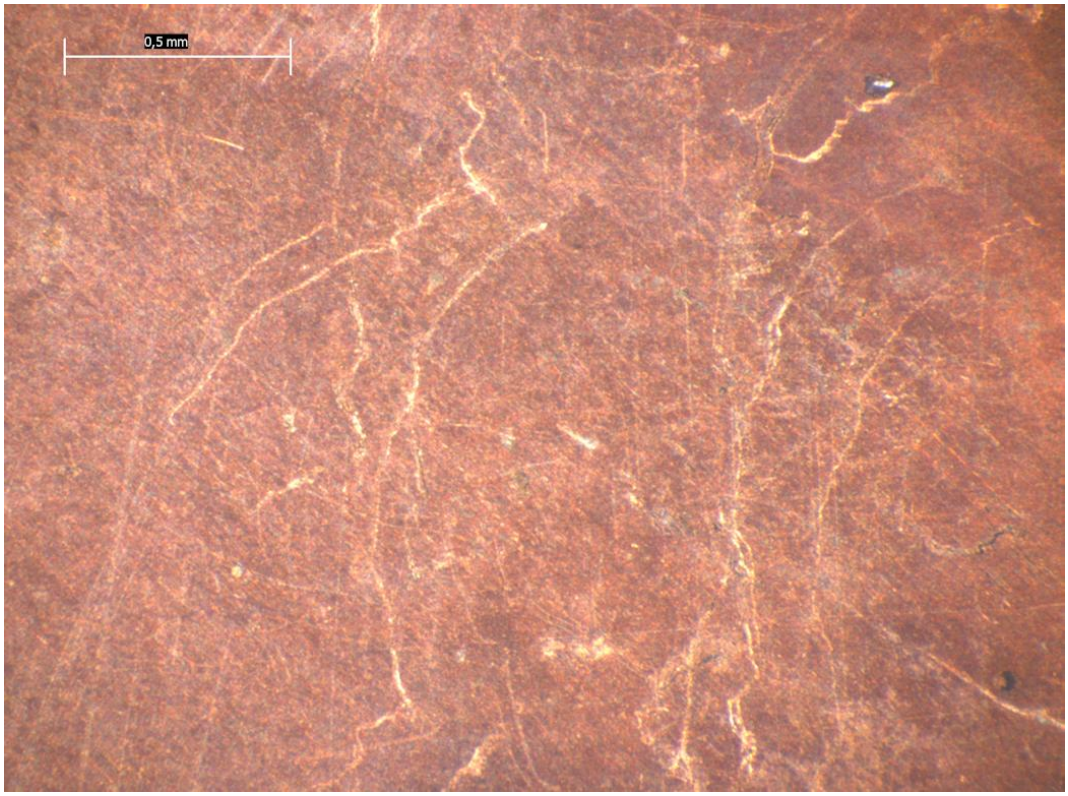

Figure 8: Higher magnification stereomicroscope image of features in bar Cu8, said to be cracks initiated during the test.

3.1 SEM examinations of specimens

In order to estimate specimen quality, prepared TEM specimens were examined in SEM. In all cases, it was found that the specimens contained parallel stringers of second phase material, oriented along the axis of the test bars. An example from specimen Cu5_4 is shown in Figure 9, and a higher magnification image of similar stringers in Cu8_1 is shown in Figure 10. During electropolishing the interface between the matrix and stringers typically experienced preferential attack, leading to a significant amount of particle drop-out in the thin, electron-transparent material.

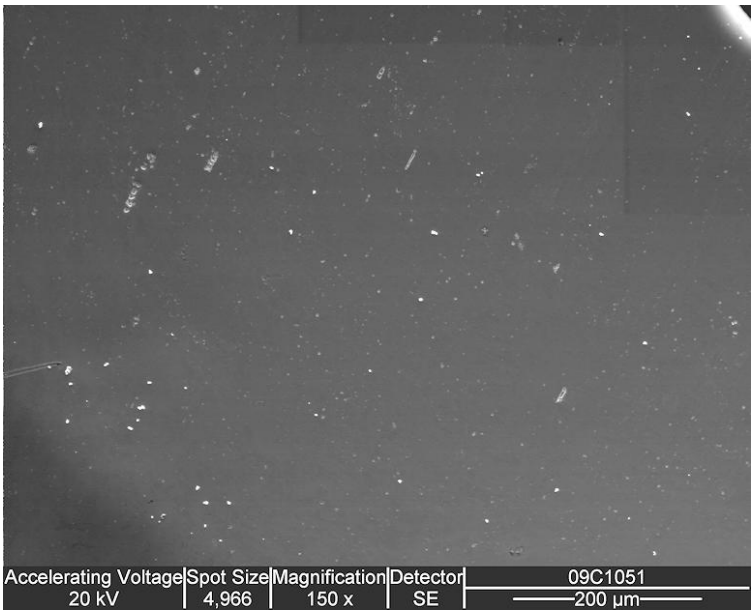

Figure 9: Stringers of second phase are readily apparent in the electropolished materials, as in this example from specimen Cu5_4.

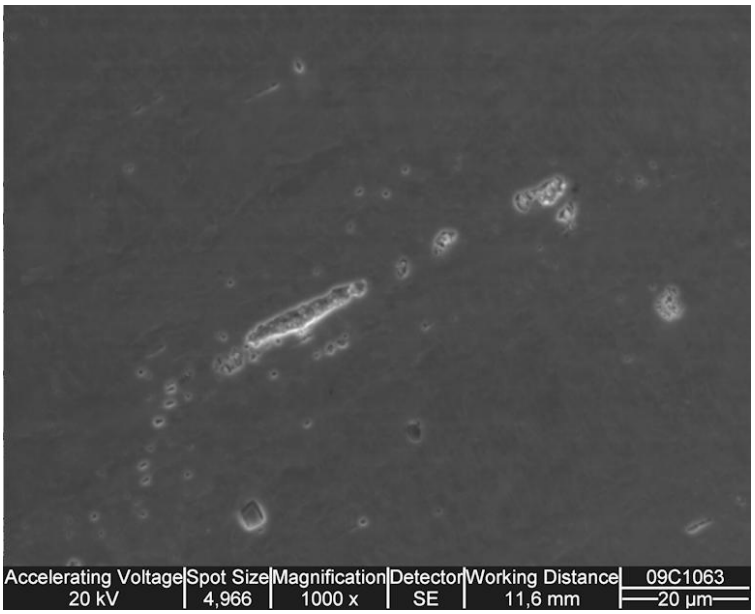

Figure 10: Higher magnification SEM image of second phase particle stringers, this time from specimen Cu8_1.

3.2 TEM results of bar Cu5

Because bar Cu5 was considered a reference specimen that was not expected to show much effect of the environment on the dislocation structure following its low level of loading, detailed examination was only conducted of specimen Cu5_6, corresponding to the centre of the gauge area. For comparison specimen Cu5_4 was also examined, but its microstructure did not differ remarkably from that of Cu5_6, so micrographs were only recorded from the latter.

3.2.1 TEM results of specimen Cu5_6

Figure 11 contains a sampling of microstructures from different regions of specimen Cu5_6. The microstructure is heavily distorted, and contains a high density of dislocations. As particularly evident in the lower left image of that figure, particle fallout occurred during specimen preparation. As shown in Figure 12, one isolated grain was found which contained a remarkably low density of dislocations. Analysis of the composition of the grain showed it to be pure copper.

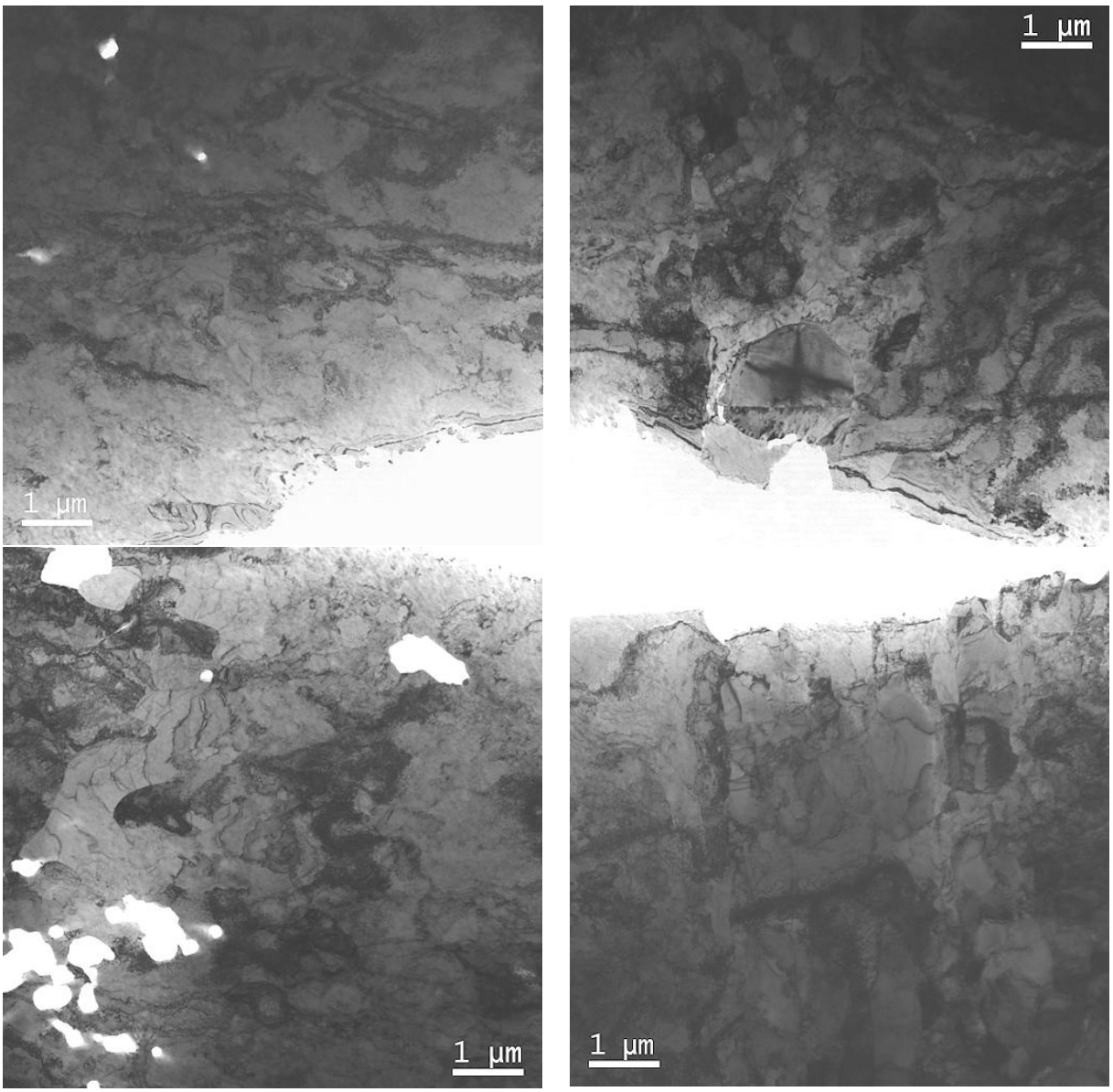

Figure 11: A sampling of microstructure from different regions of specimen Cu5_6.

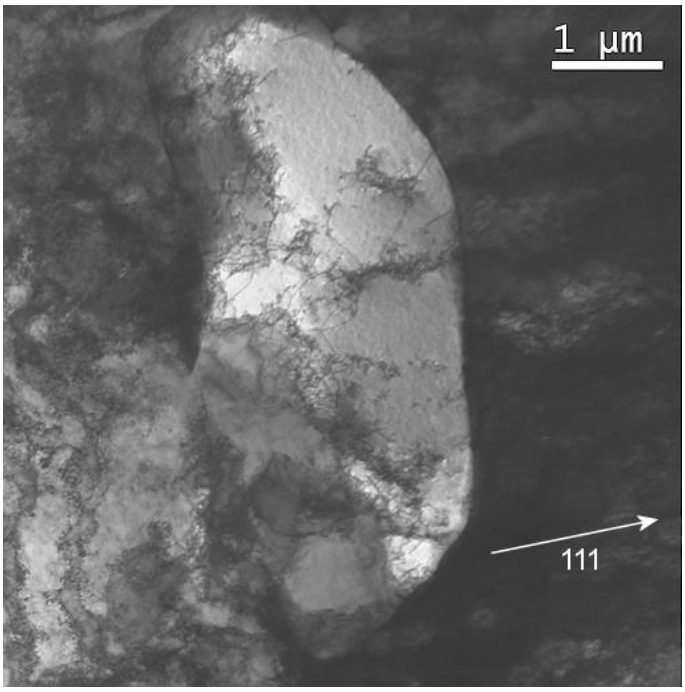

Figure 12: An isolated grain within Cu5_6 having a remarkably low density of dislocations.

3.3 TEM results of bar Cu6

The microstructure of bar Cu6 was examined from locations 2, 3 and 4. The first of the series examined was Cu6_3, and when it showed remarkable results, specimens Cu6_2 and Cu6_4 were also examined to offer comparisons.

3.3.1 TEM results of specimen Cu6_3

Figure 13 contains a sampling of microstructures from different regions of specimen Cu6_3. In most regions the microstructure was similar to that of bar Cu5. However, remarkable in Cu6_3 was the existence of particular grains which appeared to have no dislocations, an example of which is visible in the lower right image of Figure 13. Such regions were examined more carefully. Although in appearance they resembled a second phase inclusion, energy dispersive x-ray spectroscopy (EDS) revealed that they were comprised of pure Cu. Because they contained very little oxygen, they could not be considered to be oxide inclusions. Figure 14 is a higher magnification image of the same grain visible in the lower right image of Figure 13, but now tilted to a diffraction condition that should bring the dislocations in the material into contrast. It reveals a dislocation-free matrix having a diffraction pattern consistent with that expected for metallic copper, a well-defined boundary, and outside of the grain a dislocation density that is quite high. Whereas the 111-type reflection shown in selected area diffraction (SAD) pattern 22 of that figure should reveal half of the dislocations present, the 002-type reflection shown in SAD pattern 23 for the dislocation-free grain would be expected to reveal 2/3 of the dislocations present. Clearly such regions represent islands of dislocation free material within the surrounding highly deformed matrix. By contrast, Figure 15 shows how densely the dislocations are distributed in the rest of the material.

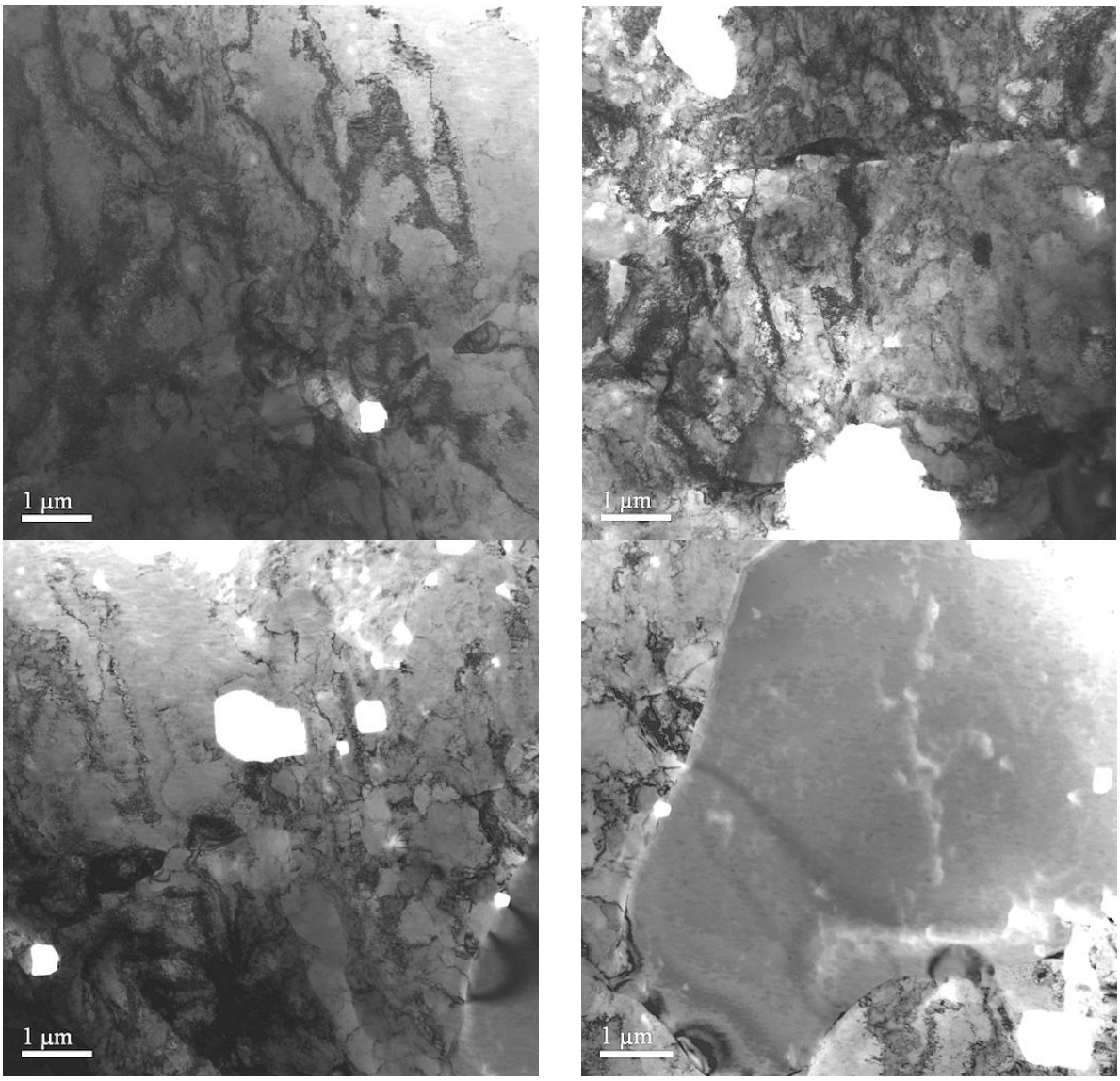

Figure 13: Sampling of microstructure in specimen Cu6_3.

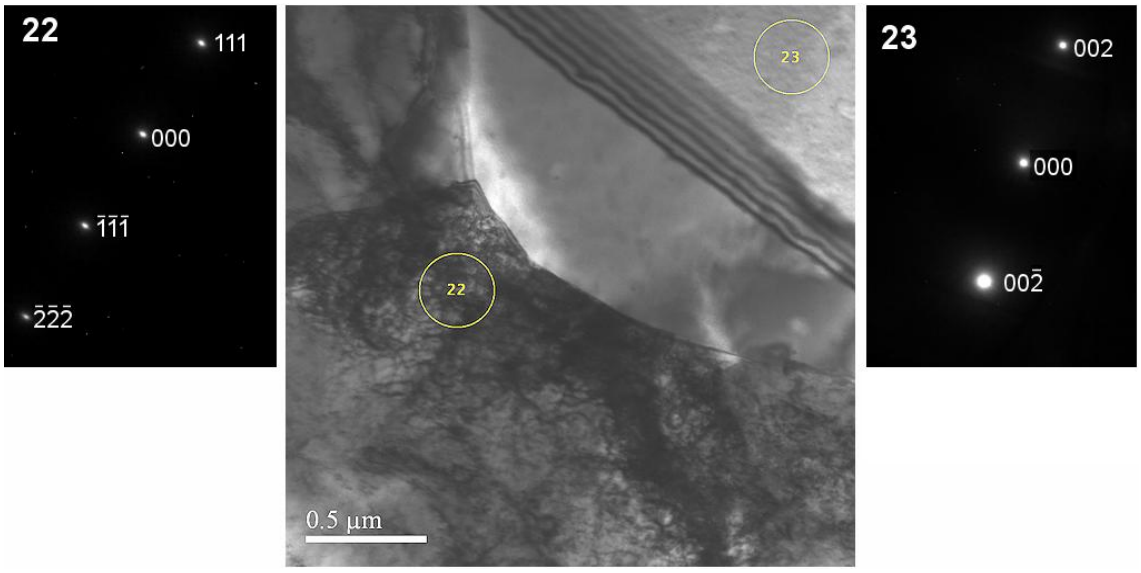

Figure 14: Tilted to conditions to reveal dislocations, it is evident that within the grain there are no dislocations, while outside it the density of dislocations is very high.

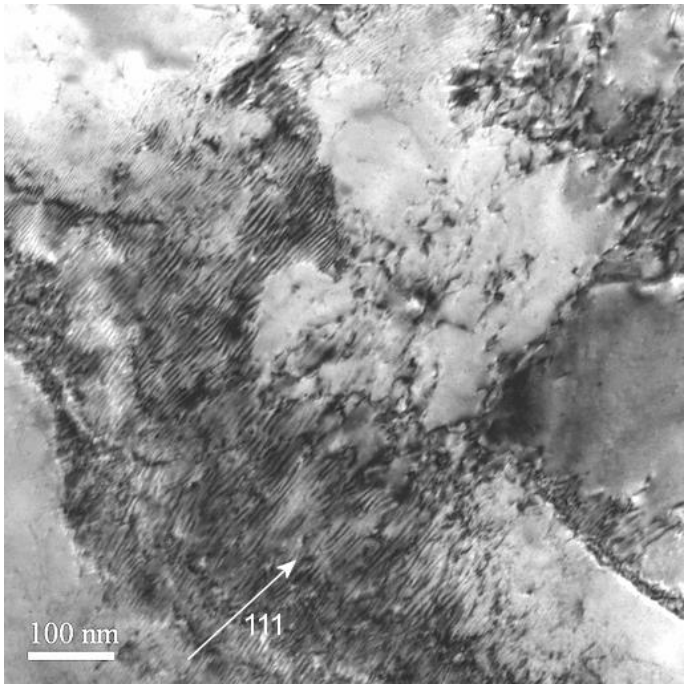

Figure 15: High magnification image of dense mat of dislocations typical of the material outside of dislocation free grains.

3.3.2 TEM results of specimen Cu6_2

Because of the uniqueness of the dislocation-free grains found within specimen Cu6_3, its pair from the same region of the test bar was also examined. Figure 16 contains a sampling of microstructures from different regions of specimen Cu6_2. The principle finding from that specimen is that very few, if any, dislocation-free grains were apparent as manifested in Cu6_3. However, one feature that may be noteworthy is the band about 3 microns wide that is visible in the upper left-hand image of Figure 16.

3.3.3 TEM results of specimen Cu6_4

Because of the discrepancy between Cu6_2 and Cu6_3 regarding the presence of dislocation free grains, specimen Cu6_4 was also examined. Its location at the gauge region of the test bar also made it interesting from the standpoint that the stress would be expected to be greatest in this region during the test. Figure 17 contains a sampling of microstructures from different regions of specimen Cu6_4. At that magnification the microstructure is similar to that of Cu6_2. At a higher magnification, as shown in Figure 18, the dislocation structure may by slightly less dense. However, since the density is overall still quite high, it is difficult to assess the extent of such a reduction in density on a broad basis. Most importantly, no dislocation free grains were found of the kind observed in Cu6_3.

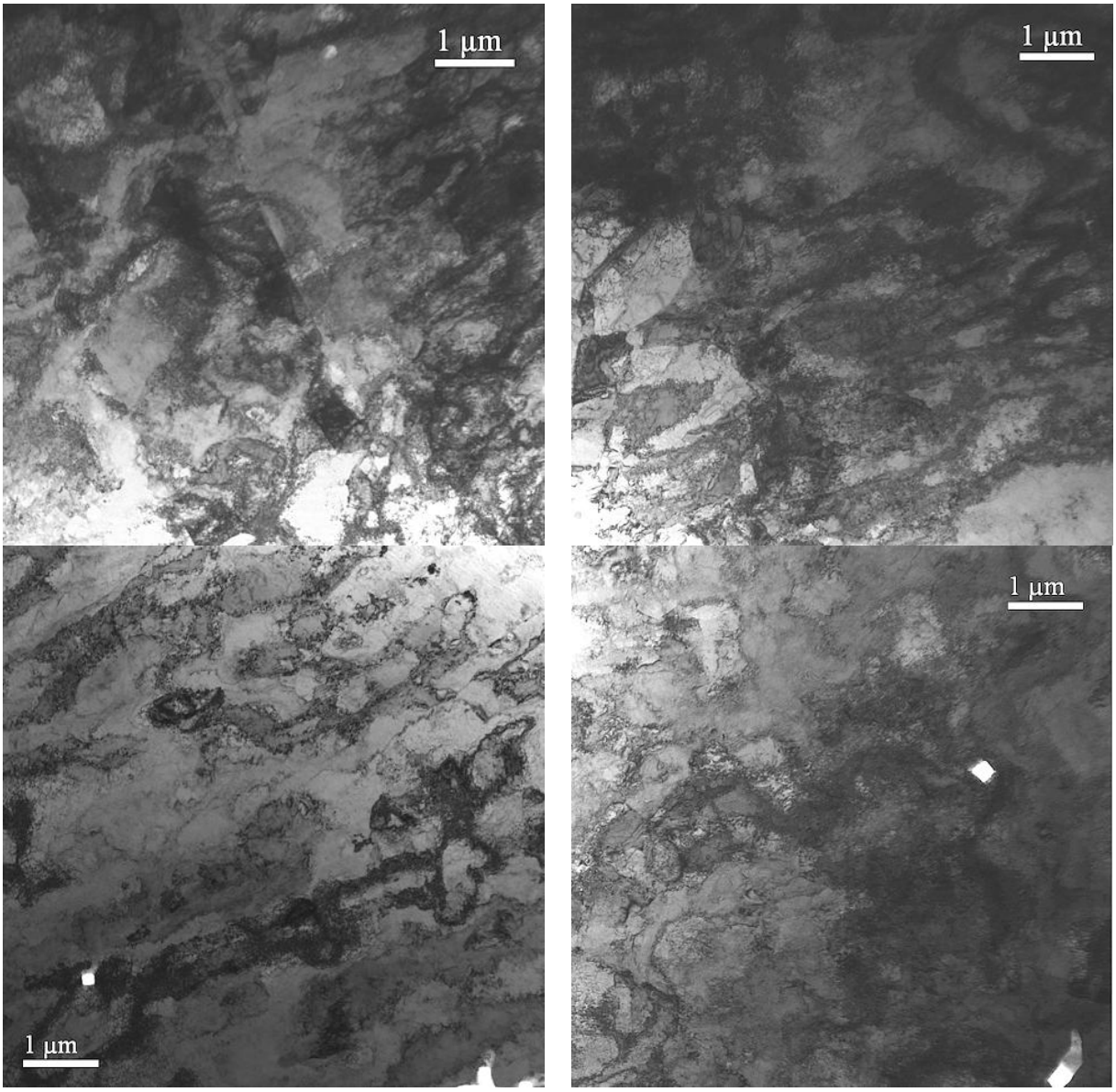

Figure 16: Sampling of the deformation microstructure in specimen Cu6_2.

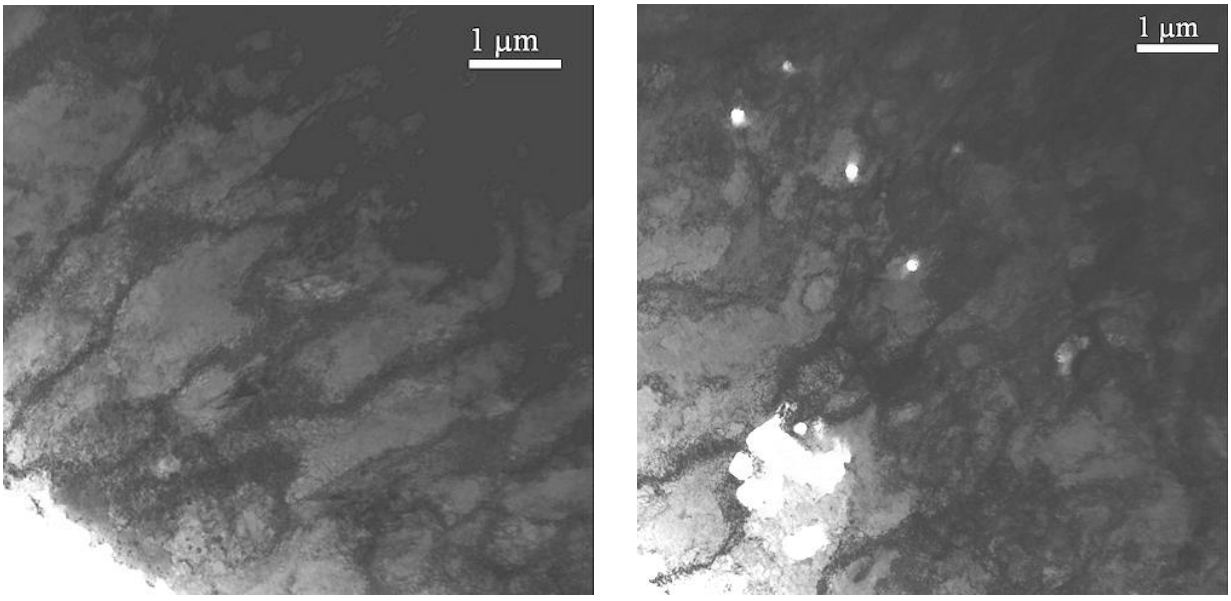

Figure 17: Sampling of the deformation microstructure within specimen Cu6_4.

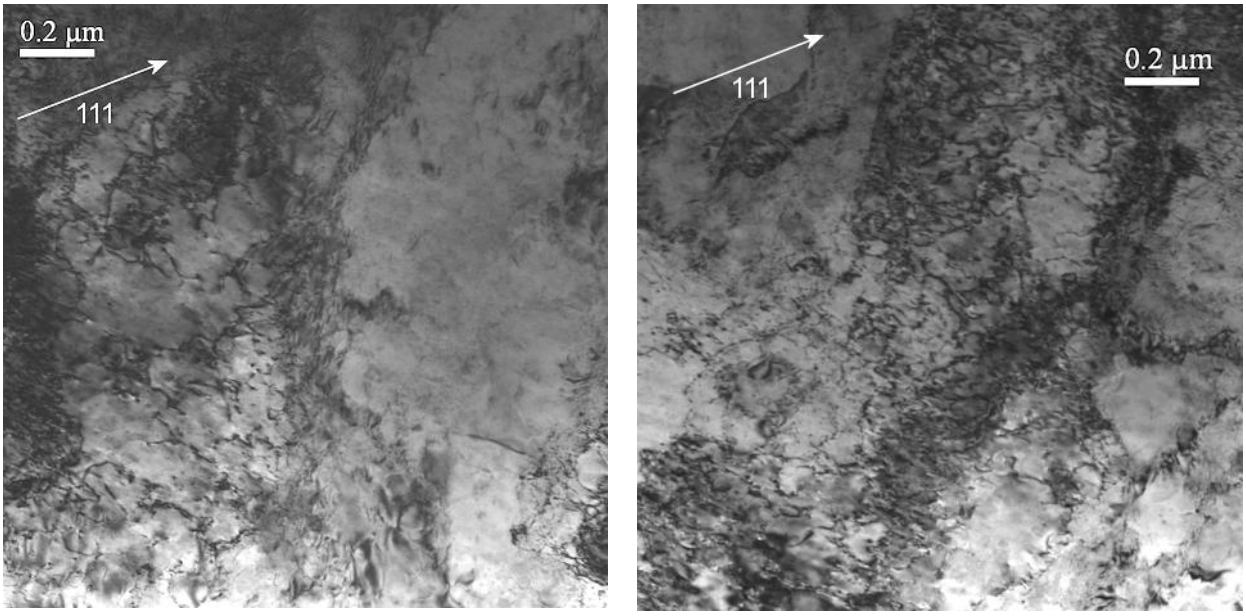

Figure 18: Higher magnification images of dislocation microstructure within specimen Cu6_4. The overall dislocation distribution may be less dense than in Cu5.

3.4 TEM results of bar Cu8

Like bar Cu6, the microstructure of bar Cu8 was also examined from locations 2, 3 and 4. For comparison, a reference specimen from position 1 in the test bar was also examined, representing material which should not have been subjected to the load or environment during the test.

3.4.1 TEM results of specimen Cu8_1

Figure 19 contains a sampling of microstructures from different regions of specimen Cu8_1. At low magnification the microstructure is similar to that of the other specimens, showing a strongly distorted matrix and high dislocation density. However, when imaged at higher magnification, it was evident that the microstructure was still mostly comprised of dense mats of tightly packed dislocations, as shown in Figure 20. Because of lattice rotation, only portions of the fields are in contrast at a given tilt.

3.4.2 TEM results of specimen Cu8_2

Specimen Cu8_2 was extracted from a position comparable to that of Cu6_2 and Cu6_3, in the deformed region outside of the gauge region. Figure 21 contains a sampling of microstructures from different regions of the specimen. For the most part the microstructure appeared similar to that of the other materials at low magnification, showing a heavily distorted lattice. In the upper right-hand image of Figure 21 a 3 micron wide band is visible, similar to that observed in Cu6_2. Several particles were also found in this specimen that were amenable to EDS analysis. It consistently showed them to be comprised of copper and oxygen, with the Cu:O ratio approximately 2:1. Meanwhile, when viewed at higher magnification, several areas were found in Cu8_2 that seemed to have a remarkably reduced density of dislocations, as shown in Figure 22.

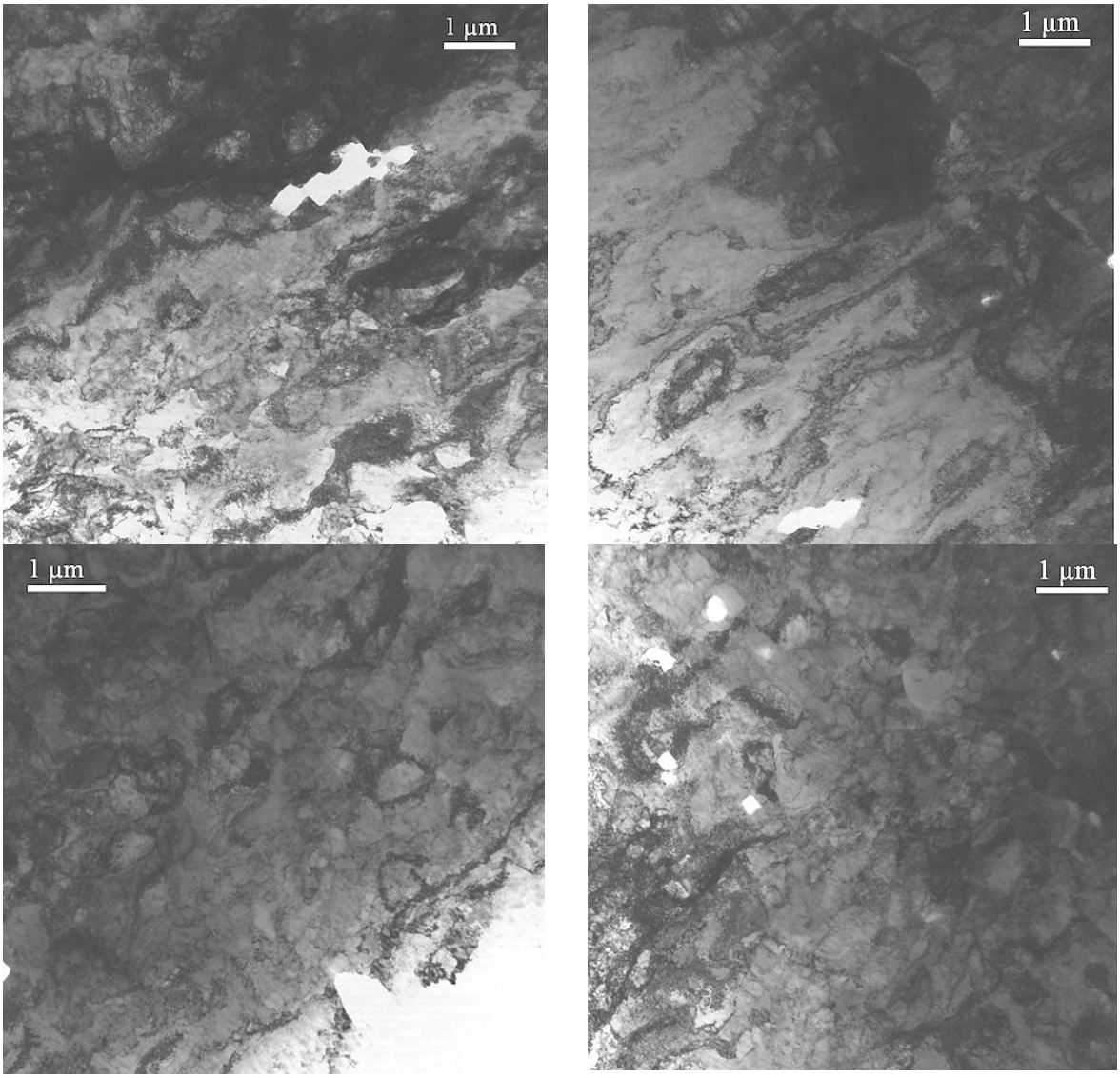

Figure 19: Sampling of microstructure within specimen Cu8_1

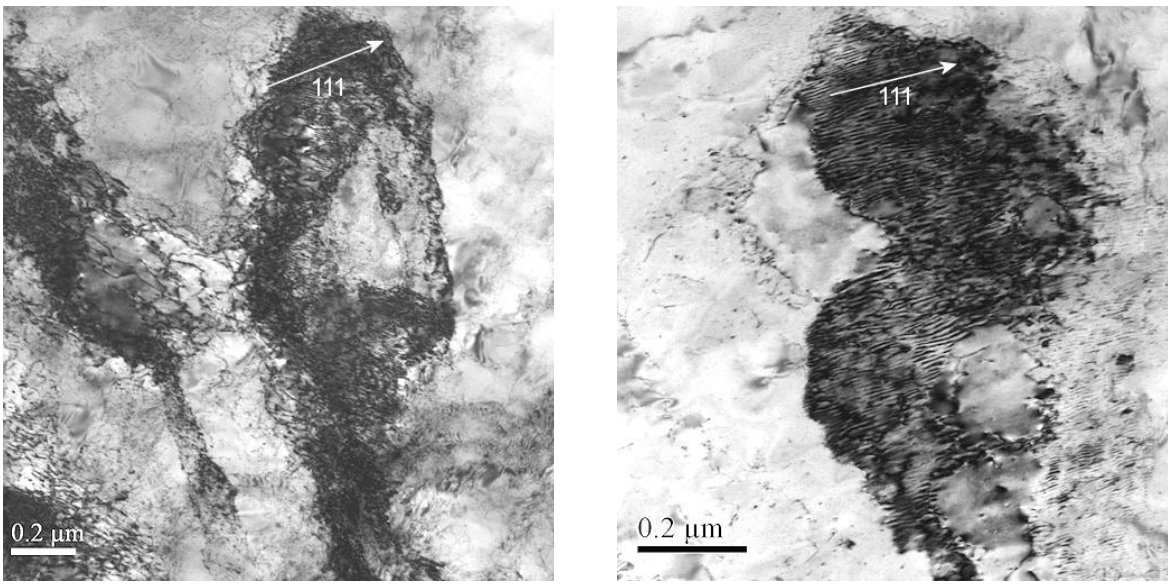

Figure 20: Higher magnification image of dense rafts of dislocations in Cu8_1. Because of lattice rotation, only portions of the fields are in contrast at a given tilt.

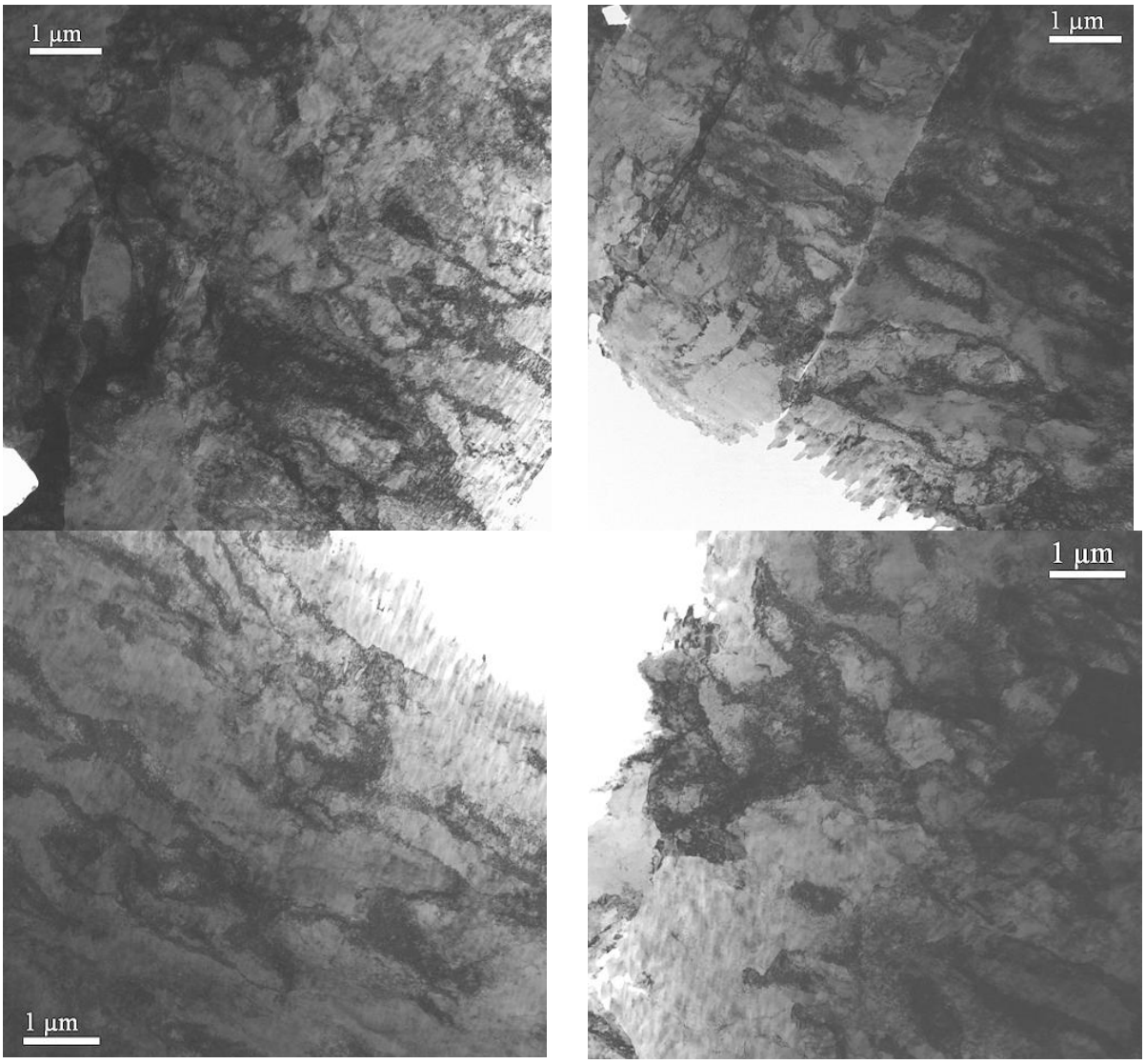

Figure 21: Sampling of deformation microstructure within Cu8_2.

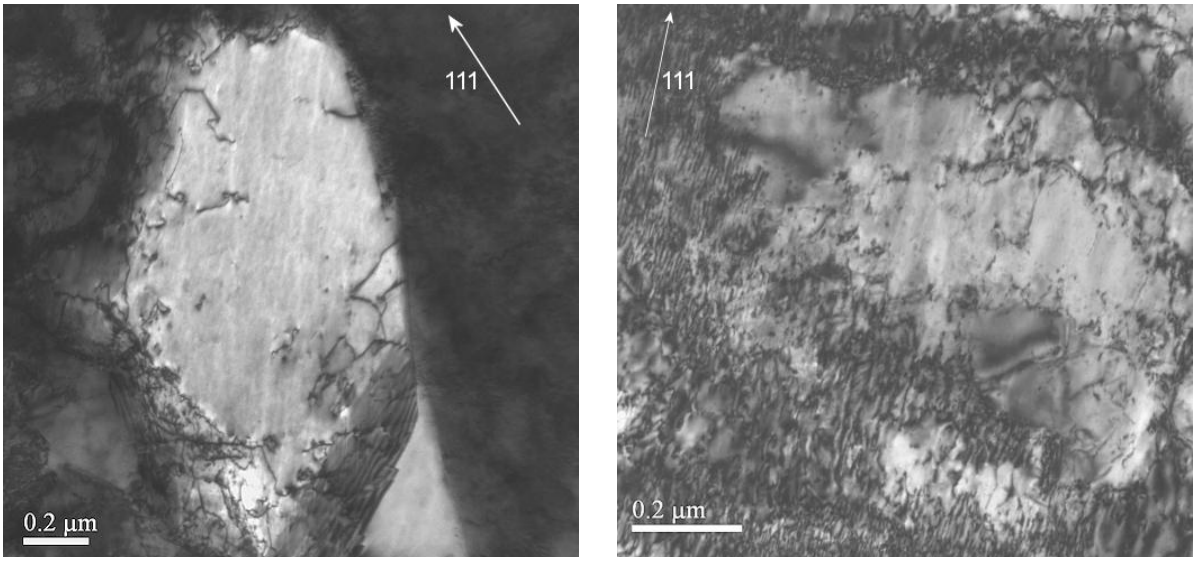

Figure 22: At higher magnification, one small grain in Cu8_2 appeared to have a dramatically reduced density of dislocations (left), and other areas also appeared to exhibit reduced dislocation density (right).

3.4.3 TEM results of specimen Cu8_3

Specimen Cu8_3 is the pair to Cu8_2, from the deformed area outside the gauge region of the test bar. Figure 23 contains a sampling of microstructures from different regions of the specimen. For the most part the microstructure appeared similar as that of other specimens. However, as shown in the lower right image of Figure 23, some grains were also found which appeared to have a reduced dislocation density. This is shown more clearly at higher magnification in the left-hand image of Figure 24. However, such regions were still an exception, with most of the microstructure still being comprised of mats of densely packed dislocations, as shown in the right-hand image of Figure 24.

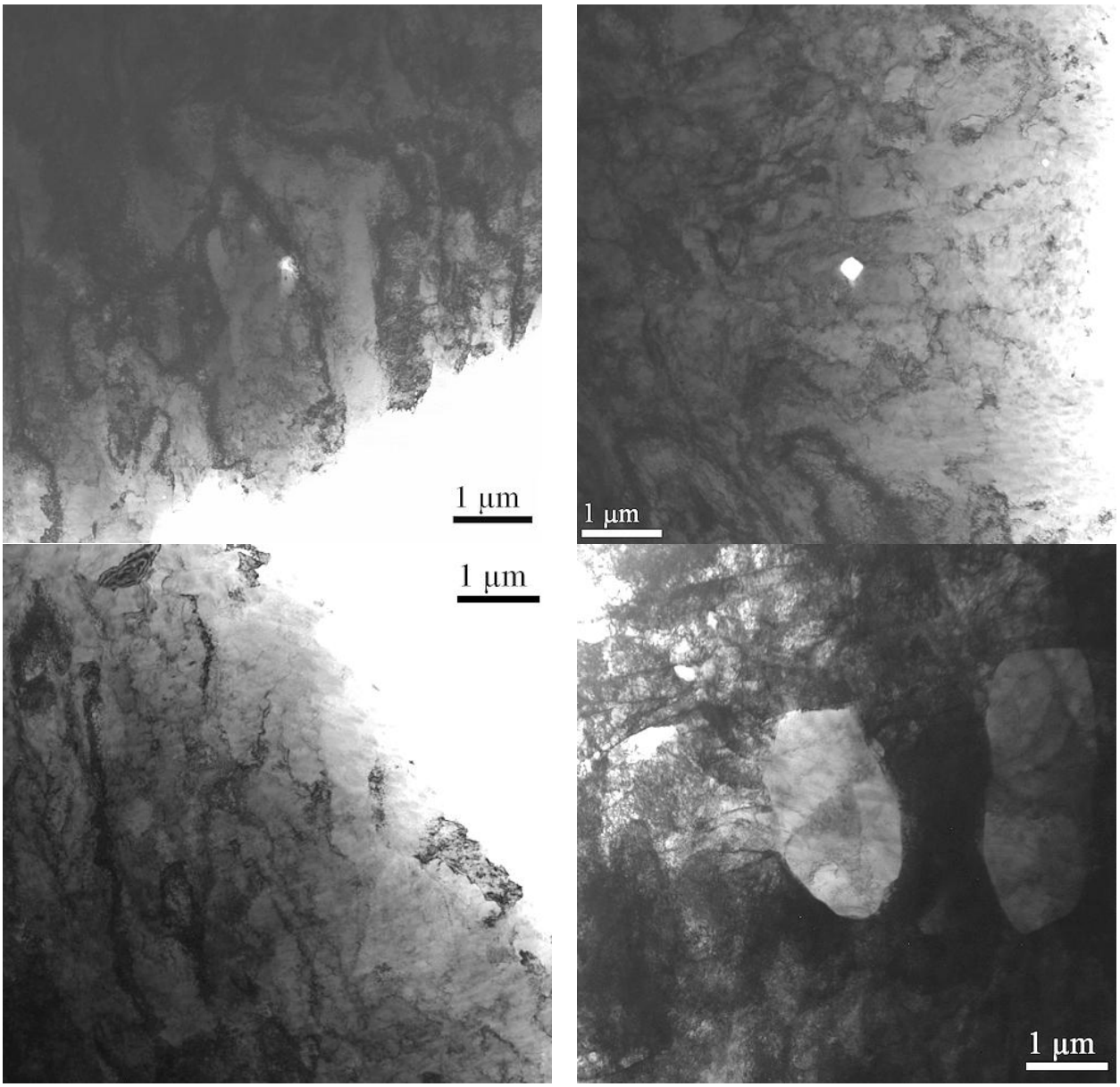

Figure 23: Sampling of deformation microstructure within Cu8_3.

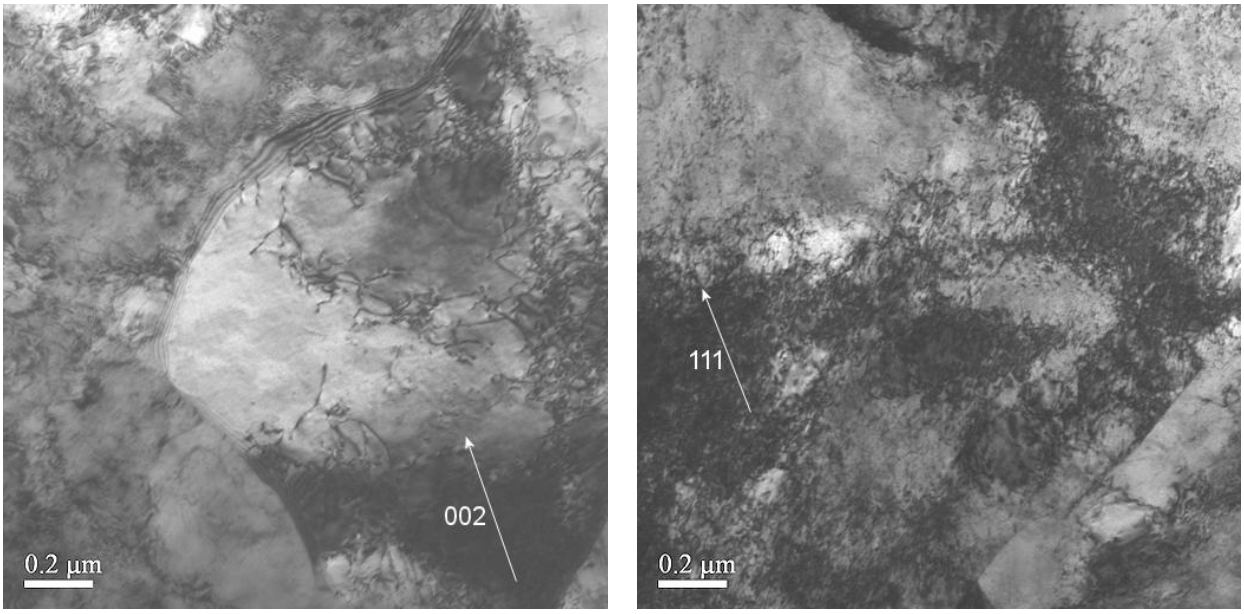

Figure 24: Higher magnification images of a grain showing reduced dislocation density (left) and a more typical region of a dense mat of dislocations (right).

3.4.4 TEM results of specimen Cu8_4

Like Cu6_4 and Cu5_6, specimen Cu8_4 was from the gauge region of bar Cu8. Figure 25 contains a sampling of microstructures from different regions of specimen Cu8_4. Although in many ways quite similar in appearance to that of the other specimens, it seemed that the microstructure of specimen Cu8_4 may have exhibited more grains having reduced dislocation density than in the other specimens (with the exception of Cu6_3.) Some examples of those regions are shown at higher magnification in Figure 26. Overall, therefore, it would seem that the deformed regions of bar Cu8 may have exhibited a marked reduction in dislocation population in many regions, albeit still exhibiting a substantial amount of heavily deformed material in most regions.

4 Discussion

Three different test bars were subjected to different combinations of strain and electrochemical polarization in EAC tests. Post-test stereomicroscope examination found that when a bar was loaded at only 50 MPa, the surface of the specimen had turned black, but when loaded at 250 MPa some corrosion product and pitting were visible on the surface but the test bar still remained mostly copper coloured. Finally, at 320 MPa some features appeared on the specimen which could be interpreted to be cracks, despite occurring outside of the gauge region. The material was considered to be commercially pure copper, but specimens prepared by electrolytic means revealed stringers of second phase particles in all the test-bars, oriented parallel to the test-bar axis. In TEM specimens still retaining distinct particles within the matrix, EDS analysis confirmed them to be copper oxide particles having a Cu:O atomic ratio of 2:1. They are most likely Cu_2O inclusions from the original slag formed during billet production, distributed as axial stringers in the material during subsequent rolling processing. Their affect on the test is not known, but it may be negligible.

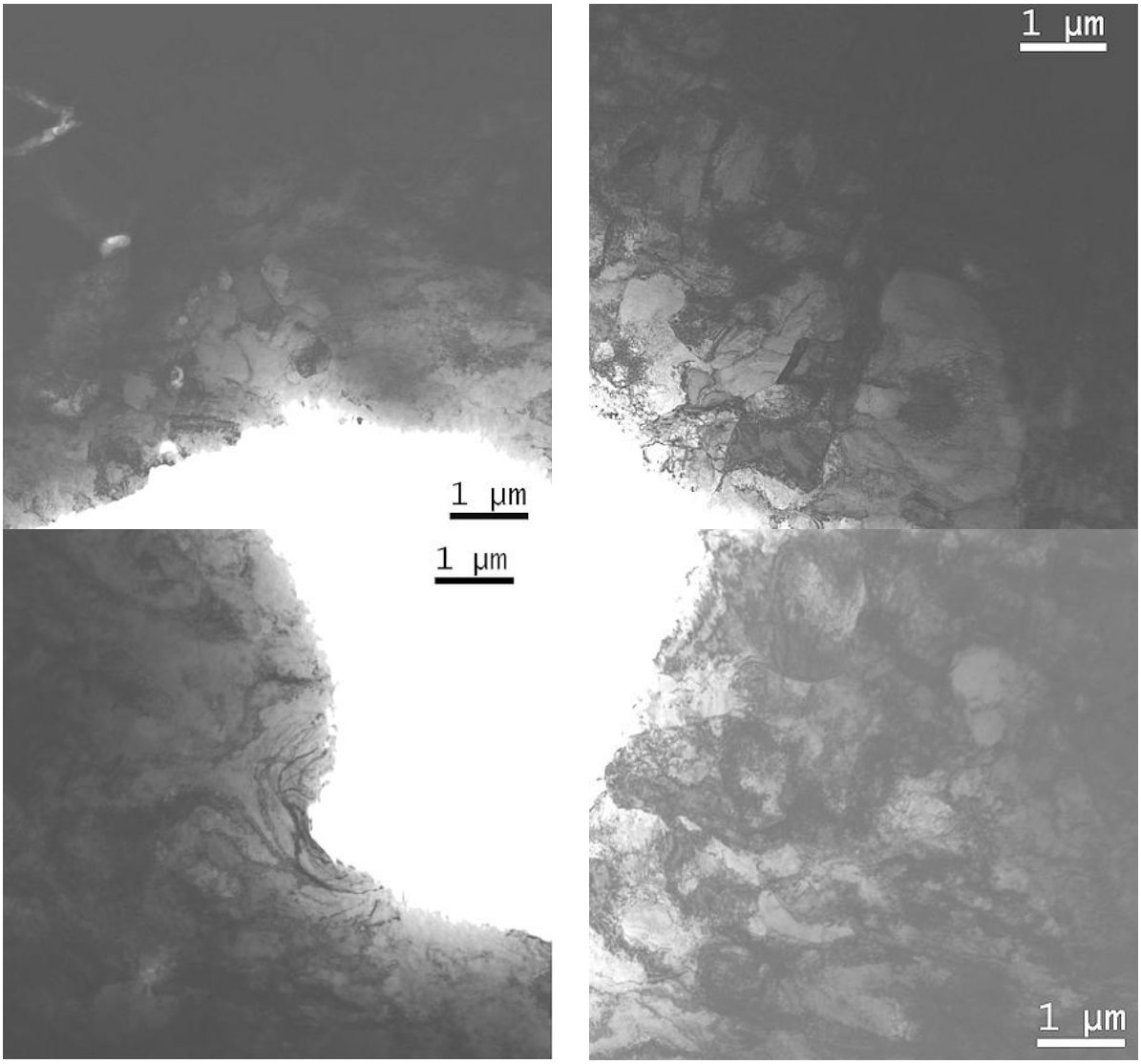

Figure 25: Sampling of microstructure within Cu8_4. Several grains appear to have a reduced density of dislocations.

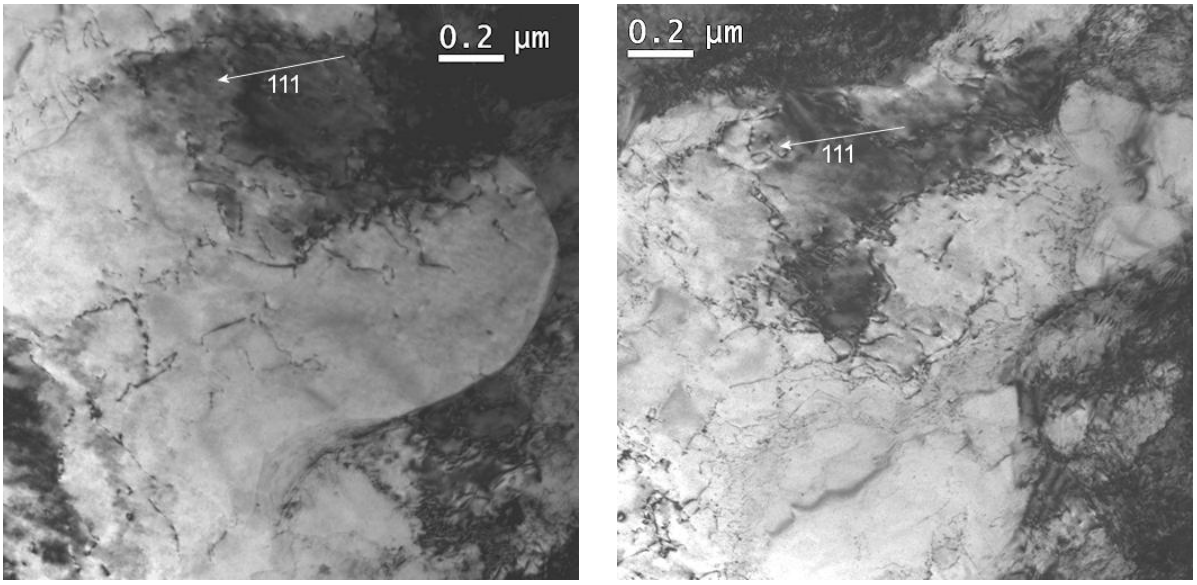

Figure 26: Higher magnification images of regions of reduced dislocation density. Such regions were more readily observable in Cu8_4.

TEM examinations conducted from different regions of the three different test bars, each corresponding to a different combination of stress and environment, yielded very little dramatic difference between them. In all cases the majority of the microstructure in each specimen was comprised of a heavily distorted lattice bearing a high density of dislocations organized as dense mats of closely-spaced, parallel dislocations.

However, most dramatically evident in specimen Cu6_3, and also found to varying extents in other specimens, were some localized regions appearing to exhibit a marked absence of dislocations, generally bounded by distinct boundaries. Such features formed what were essentially dislocation-free grains within the surrounding material exhibiting the high density of dislocations. EDS of the regions consistently showed them to be 100% copper, and SAD of the grains generally returned the same kind of diffraction pattern as the rest of the material, ruling out the possibility that they could be second phase particles of some sort. In particular, those particles which were indeed oxides were accompanied by significant dissolution of the matrix at their boundary, usually leading to fallout of the particle itself already during specimen preparation. Therefore it would seem that the dislocation-free regions were an integral part of the material as a whole, just representing a local region of significantly reduced dislocation density.

Despite the overall similarity in appearance between the different cases, in a qualitative sense it seemed that the specimens from test bar Cu8 exhibited the most incidences of such dislocation-free grains, with such features found in specimens Cu8_2 and Cu8_3, as well as being even more readily observable in specimen Cu8_4 (extracted from the gauge region.) Meanwhile specimen Cu8_1, from a non-loaded region of bar Cu8 not exposed to environment, did not exhibit any such dislocation-free grains.

On the other hand, while specimen Cu6_3 clearly showed the most dramatic, wide-spread incidence of such dislocation-free regions, similar regions were difficult or impossible to find in specimens Cu6_2 or Cu6_4 from the same test bar. Meanwhile, at least one such region was *also* found in specimen Cu5_6, which was loaded at a much lower level, and therefore not expected to exhibit much deformation. Therefore, although in a qualitative sense test bar Cu8 may have exhibited more reduction in dislocation population during the test, the results were not unambiguous considering that similar observations could also be made to some extent in some regions of the other test bars, but not in a consistent manner satisfying what was expected based on the polarization and load fluctuation data.

One possible reason for the discrepancy between the observations and what was expected, is that the predicted vacancy injection and subsequent vacancy-dislocation interactions may have occurred only at the immediate surface of the specimen. Revisiting the load-drop plot for Cu8 (see *Figure 3*) shows that, in fact, the drop observed represents a change of less than 5 %. Assuming that the load drop is a consequence of material softening at the test bar surface, a drop of that magnitude would correspond to an equivalent reduction of load-carrying area of only about 2% (i.e. softening in the outer 2% of the material). Taking into account the dimensions of the gauge region cross-section, and assuming uniform interaction with the environment, the softening may have only occurred in the outer 10 microns of the specimen cross-section. Therefore, it is conceivable that the specimen preparation method employed in the current study simply examined re-

gions of the test bars that were too distant from the surface, and therefore were unsuccessful in capturing very widespread evidence of the expected manifestation. Nonetheless, the fact that the specimens from test bar Cu8 did seem to exhibit some reduction in dislocation population in some regions matches expectations to some degree. Likewise, it is conceivable that the specimen blank of Cu6_3 may have been mechanically thinned to a greater extent than other blanks, with the region of subsequent examination being closer to the surface. Finally, it is possible that the preparation of additional specimens focused only on the immediate sub-surface region could enable observations that would more closely match what was expected. One means for this would be the utilization of the focused ion beam (FIB) method to prepare TEM specimen cross-section of the oxide, its interface with the matrix, and the matrix region immediately below the oxide, where the most vacancy/dislocation interaction would be expected to occur.

5 Summary and Conclusions

In the selective dissolution, vacancy creep model it is postulated that corrosion processes at a material surface can, in some conditions, result in an overall net increase in vacancy flux from the oxide into the bulk metal. Vacancy injection is expected to promote dislocation activity, and subsequent dynamic recovery would be expected to soften the material locally. This could be viewed as a key precursor process for stress corrosion crack initiation. The goal of the current study was to utilize transmission electron microscopy (TEM) to examine the dislocation microstructure of tested materials following different test outcomes, in order to determine whether or not dislocation activity was significantly different following different test sequences.

Three different test bars were subjected to different combinations of strain and electrochemical polarization in EAC tests. TEM examinations conducted from different regions of the three test bars, each corresponding to a different combination of stress and environment, found only some differences between them. In all cases the majority of the microstructure in each specimen was comprised of a heavily distorted lattice bearing a high density of dislocations organized as dense mats of closely-spaced, parallel dislocations. However, some localized regions appeared to exhibit a marked absence of dislocations, generally bounded by distinct boundaries, but still showing 100% copper in analyses. In a qualitative sense it seemed that the specimens from test bar loaded to 320 MPa (exceeding the nominal yield strength of the material) exhibited the most incidences of such dislocation-free grains, being found in all three deformed regions examined. On the other hand, while one specimen from the deformed material of the bar loaded at 250 MPa clearly showed the most dramatic, wide-spread incidence of such dislocation-free regions, similar regions were difficult or impossible to find in other specimens from deformed material in the same test bar. Meanwhile, at least one such region was *also* found in the gauge region of the test bar that was loaded at only 50 MPa, and therefore not expected to exhibit much deformation.

Calculations show that is possible that the predicted vacancy injection and subsequent vacancy-dislocation interactions may have occurred only at the immediate surface of the specimen though, so preparation of additional specimens focused only on the immediate sub-surface region could enable observations that would more closely match what was expected.